Fachtagung "Lasermethoden in der Strömungsmesstechnik"
8. – 10. September 2015, Dresden

Numerische Untersuchungen von Windkraftanlagen: Leistung, Wake und Steuerungsstrategien

Numerical Investigations of Wind Turbines: Performance, Wake and Control Strategies

Ali Al-Abadi[1,2], Özgür Ertunç[3], Youjin Kim[4], Jin-young Park[4], Frederik Berger[5] & Antonio Delgado[1,4]
[1]Institute of Fluid Mechanics, Friedrich-Alexander-University, Erlangen, Germany
[2]AlKhwarizmi College of Engineering, University of Baghdad, Baghdad, Iraq
[3]Ozyegin University, Mechanical Engineering Department, Istanbul, Turkey
[4]Institute of Fluid Mechanics, Friedrich-Alexander-University Busan, South Korea
[5]Institut of Physics, Carl von Ossietzky University, Oldenburg, Germany

Schlagworte: Numerische Simulation, Windturbinen, Leistung, Steuerungsstrategien, Wake
Key words: Numerical simulation, Wind turbines, Performance, Control-strategies, Wake

Abstract

In this study, numerical investigations of the performance, wake and control-strategies of an optimized wind turbine were performed. These investigations delivers an intensive insight of the wind turbine operation under different control strategies. Further, wake analysis has been validated with existing experimental data. The wind turbine was analyzed by the 3-D steady state CFD simulations of Star CCM+ and by using of two CFD configurations. These are wake and pitch models. The first is used for the wake analysis at the design velocity, whereas the second, which is constructed of the overset technique, is applied for the pitch-control strategy. The overset mesh technique was adapted in the pitch model to overcome the computational domain with overlapping grids. The main advantage of the overset is to facilitate the computational time and effort in investigating the pitch control-strategy, since the pitch angle is prone to variation within a range of operating speed. Thus, it is possible to predict the performance and show a constant output rated power. The wake analysis results show agreement with the experimental data.

Introduction

The reliability of the computational analysis to study the flow over large structures, such as wind turbines without the need for scaling has been proven in enormous studies. However, the quality and effectiveness of the computations are dependent on the applied physical models. Furthermore, computational methods involve many turbulent models to solve different flow structures [1]. The k-ω Shear Stress Transport (SST) turbulence model was proven to perform well in wind turbines, since it consider the rotational effects [2,3].

In the present study, intensive numerical investigations of performance, wake and control strategies for validation of an optimized turbine were performed. Steady state RANS with the k-ω SST turbulence model were used in the numerical simulations. The performance at different operation points and the wake at the design point were investigated and compared with experimental data. In order to study the pitch-control strategy, the overset technique in Star-CCM+ was used to overcome the variable pitch angle without losing of the fidelity of the mesh.

Numerical Setup

A wind turbine rotor geometry, which was optimized with using TMASO method [4], is validated with the numerical simulation. The geometry files were imported to Star CCM+ as IGES. The computational domain was chosen to be cylindrical. The simulations of the three bladed horizontal axis wind turbine (HAWT) were performed as steady state simulations, with a geometrically constant inlet wind velocity. Thus, it is possible to apply the periodic boundaries to the model. The simulation of a 120° fraction of a cylindrical domain with one blade was used. The dimensions are normalized to the wind turbine rotor radius R=0.25m. The interfaces faces with the outer domain and the periodic are shown in Figure 1(a).

Figure 1(b) shows the overset grid configuration. The blade geometry was enclosed and subtracted from the overset domain. The geometry of the domain is designed to fit in the inner domain. The overset domain was connected with the inner domain mesh by an overset grid interpolation. This has an advantage of moving relative to the inner domain without changing of the geometry files and the mesh. The hub was removed from the overset domain to allow flexible moving without intersections with the outer domain.

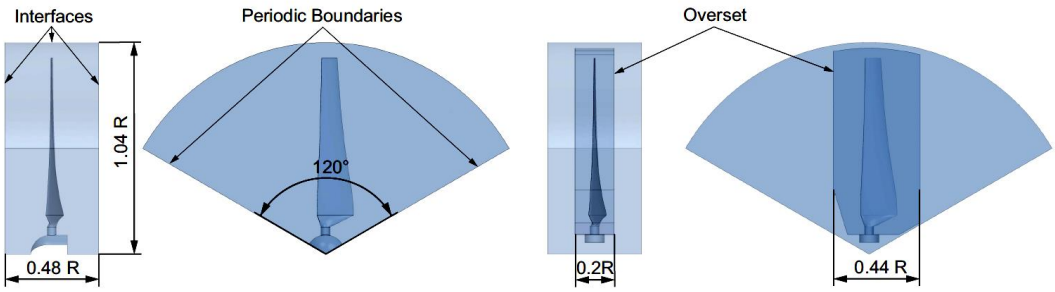

(a) Wake model (b) Overset model

Figure 1: inner domain configurations

The grids were generated within the CFD program Star CCM+. The volume mesh consists of polyhedral elements with prisms for walls, where boundary layers form.

The surface mesh size is set by the base size of the domain. For surfaces of interest this value can be adjusted. Here the surface size for the in-place interfaces of the outer domain and the surfaces of the blade are adjusted. The blade surfaces are shown in Figure 2.

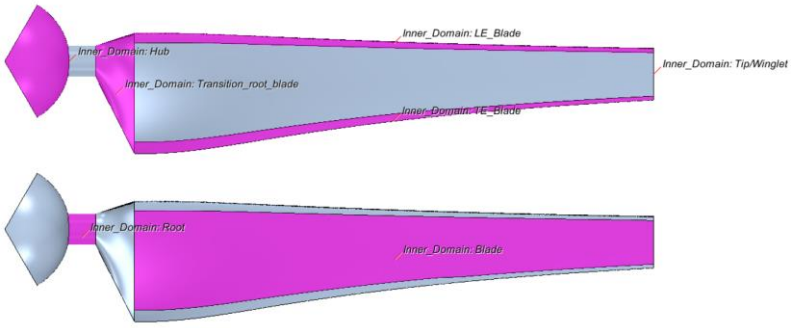

Figure 2: Surface definition on blade

Two different models and thus meshes were used for the investigations of different aspects. For the wake analysis a model with hub is used (wake model), that has two domains (outer and inner domain). Further, a model with variable pitch angle (pitch model) was tested. In this model the hub is neglected and a third domain, the overset domain, is used. The polyhedral volume mesh size is defined by the base size. Adjustments are made by volumetric controls that are presented by CAD volumes.

Main mesh settings were defined globally for all domains. The adjusted surface mesh sizes and volumetric control sizes, in ratio to the base size, are shown in Table 1 for the wake model and in Table 2 for the variable pitch model. The number of cells and faces for the eight models is stated in Table 3.

Table 1: Mesh parameters for wake model

Outer Domain	Base size:	0.07m
Surface size	Minimum surface size [%]	Target surface size [%]
In place interfaces	10	10
Volumetric control	Size [%]	
Far wake	20	
Inner Domain	Base size:	0.007m
Surface size	Minimum surface size [%]	Target surface size [%]
LE_Blade	2	4
TE_Blade	2	4
Tip/Winglet	2	4
Blade	4	10
Trans_root_blade	4	10
Root	8	32
Hub	8	32
Volumetric control	Size [%]	
Near Wake	12	

Table 2: Mesh parameters for pitch model

Outer Domain	Base size:	0.07m
Surface size	Minimum surface size [%]	Target surface size [%]
In place interfaces	10	10
Volumetric control	Size [%]	
Far wake	20	
Inner Domain	Base size:	0.007m
Volumetric control	Size [%]	
Overlap Refinement	50	
Overset Domain	Base size:	0.007m
Surface size	Minimum surface size [%]	Target surface size [%]
LE_Blade	2	4
TE_Blade	2	4
Tip	2	4
Blade	4	10
Trans_root_blade	4	10
Root	8	32
Overset	50	50
Volumetric control	Size [%]	
Near Wake	12	

Table 3: Mesh cell and face count

Model	**Outer** Cells $[10^6]$	**domain** Faces $[10^6]$	**Inner** Cells $[10^6]$	**domain** Faces $[10^6]$	**Overset** Cells $[10^6]$	**domain** Faces $[10^6]$	**Overall** Cells $[10^6]$	Faces $[10^6]$
Wake	0.98	6.83	3.03	15.32	-	-	4.00	22.15
Pitch	0.36	2.45	0.27	1.19	4.29	20.40	4.81	24.03

The prior described models provide a complete and closed system of numerical equations for the given task. With the implementation of boundary condition values the system can be solved numerically. The values for the wake model is listed in Table 4 and for the pitch model in Table 5.

Table 4: Boundary conditions of the wake model

Outer Domain	
Inlet	Velocity inlet
Outlet	Pressure outlet
Mantle	Slip wall
Interfaces	In-place interface
Periodic boundaries	Periodic interface
Inner Domain	
Interfaces	In-place interface
Periodic boundaries	Periodic interface
LE_Blade	No-slip wall
TE_Blade	No-slip wall
Tip/Winglet	No-slip wall
Blade	No-slip wall
Trans_root_blade	No-slip wall
Root	No-slip wall

Table 5: Boundary conditions of the pitch model

Outer Domain	
Inlet	Velocity inlet
Outlet	Pressure outlet
Mantle	Slip wall
Interfaces	In-place interface
Periodic boundaries	Periodic interface
Inner Domain	
Interfaces	In-place interface
Periodic boundaries	Periodic interface
Overset Domain	
LE_Blade	No-slip wall
TE_Blade	No-slip wall
Tip	No-slip wall
Blade	No-slip wall
Trans_root_blade	No-slip wall
Root	No-slip wall
Overset	overset Mesh

The physical configurations of the model were set to three-dimensional and steady state. The RANS k-ω SST model is applied, where it is designed for the simulation of external aeronautic flows with adverse pressure gradients and separation [5].

The distance for the first boundary layer cell from the blade surface is estimated based on chord Reynolds number (Re,c). The first prism layer has a wall distance of less than the boundary layer thickness (y<δ). In steady state simulations, the movement or rotation of objects can be modelled by additional reference frames. Here, two reference frames are applied. The outer domain is in the stationary inertial lab reference frame. The Inner domain is in a rotational reference frame. The axis of the rotational reference frame is the axis of rotation.

Results and Discussions

Nine simulations were performed. The data is shown in Table 6. On the left columns the simulation input data; wind velocity v_1 and angular speed ω are listed. The torque is the output of the simulations. The tip speed ratio λ and the chord Reynolds number at a radius of r/R=0.9. The power coefficient for the different operation points are shown in the table. Where it shows the maximum power coefficient is at wind velocity of 11m/s.

Table 6.: Tip speed ratio, torque, power coefficient and Reynolds number for wind velocities 8-16 m/s at constant angular velocity ω=196r/s.

v_1 [m/s]	ω [1/s]	λ	Torque [Nm]	C_p	$Re_{c;\, r/R=0.9}$ [10^3]
8	196	6.13	0.108	0.3568	62.7
9	196	5.44	0.177	0.4087	62.9
10	196	4.90	0.255	0.4307	63.2
11	196	4.45	0.346	0.4381	63.5
12	196	4.08	0.440	0.4293	63.9
13	196	3.77	0.535	0.4102	64.2
14	196	3.50	0.613	0.3766	64.7
15	196	3.27	0.568	0.2836	65.1
16	196	3.06	0.563	0.2316	65.6

The focus in this analysis is on the axial velocity distribution in front of the HAWT and in the wake. Values of the conducted simulation are compared with experimental data [4]. The simulations were performed at the design point which is taken from Table 6 for the maximum power coefficient and using the wake model.

For the wake analysis the axial velocity was taken by means of line probes normal to the axis of rotation. A cylindrical coordinate system was utilized in the simulation, where the rotation axis is the central axis. Eight line probes were span from the axis of rotation up to a radius of r=1.4D=0.7m, with the angle of 15° between two line probes, thus covering the 120° domain. Each line probe consists of 80 equally distributed probes. The eight axial velocity values for one radius are averaged. By averaging the velocities of the equally distributed line probes the dependency for the angle, due to the steady state simulation is minimized.

The comparisons of the simulated with the experimental values are shown, starting from far up-stream the turbine moving to far down-stream beyond the turbine. The axial velocity is normalized to the oncoming wind velocity v_1. The radial position is given by y/D, where y is the radius and D the diameter of the turbine. The axial distance to the turbine is given by x/D.

The up-stream simulated axial velocities in Figures 3 to 5 show the same trends of the experimental values. The simulation however underestimates the velocity slightly.

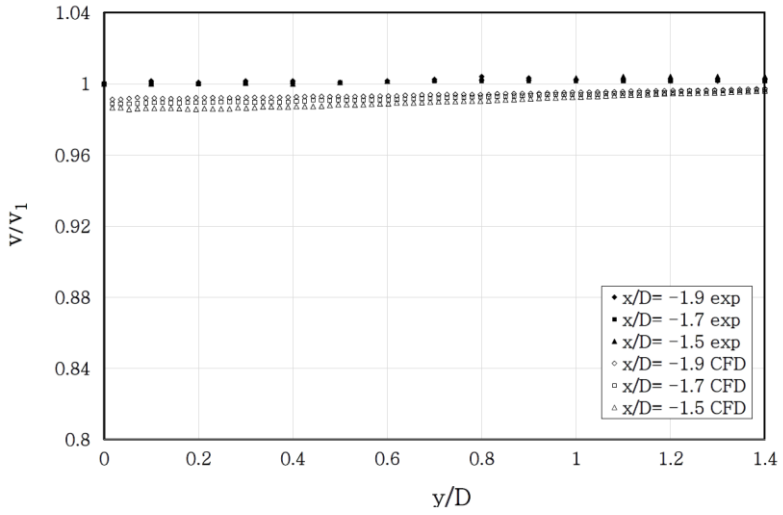

Figure 3: Axial velocity in front of HAWT in distance of 1.9 to 1.5 diameters

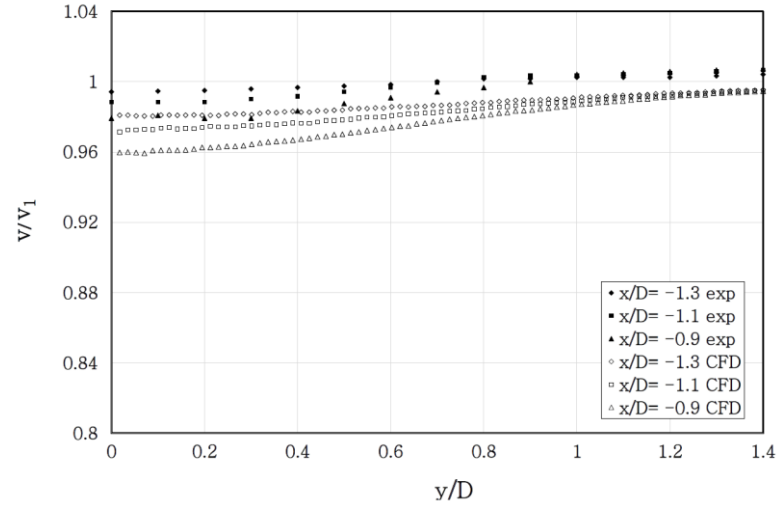

Figure 4: Axial velocity in front of HAWT in distance of 1.3 to 0.9 diameters

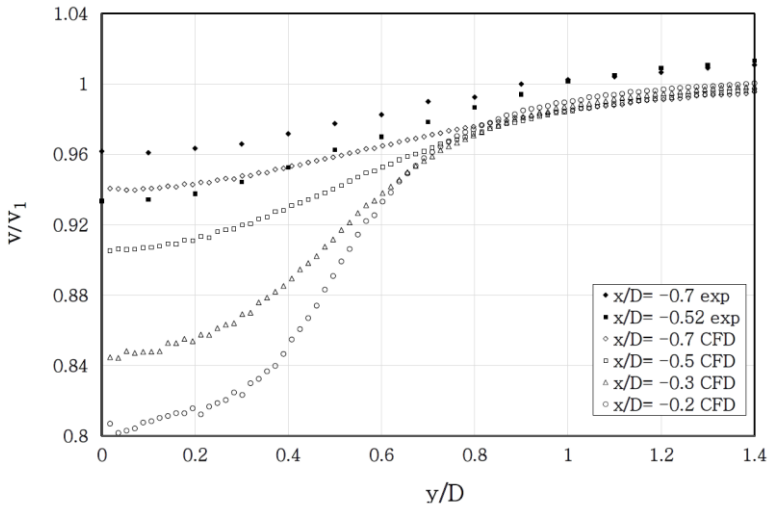

Figure 5: Axial velocity in front of HAWT in distance of 0.7 to 0.2 diameters

The velocity in the wake in a distance of 0.2 to 0.9 x/D shown in Figures 6 and 7 matches the trend of the experimental data well.

The wake velocities are underestimated, as front of the rotor. Further observation is the maximum values of the experimental wake velocity shown in the range of 0.55<y/D<0.65, is not reproduced in the simulation. These values are related to the tip vortices, which influence the flow in the wake boundary. The wake boundary forms between the wake stream tube and the outer flow. The core of the tip vortices is approximately in the middle of the wake boundary. The development of the wake boundary is associated to the tip vortices and momentum transport due to turbulence.

At distances in the wake of 1.1 to 2.1 x/D in Figures 8 to 9 the experiments show a decrease in axial velocity near the axis of rotation that is not shown in the simulation. The near axis flow is influenced by the root vortex and thus induced turbulent momentum transport. Further the transition from the wake to the outer flow is flatter for the simulation than for the experiment. This effect increases with increasing distance to the rotor. In the middle part of the wake, which is less affected by tip and root vortices the simulation follows the experimental course.

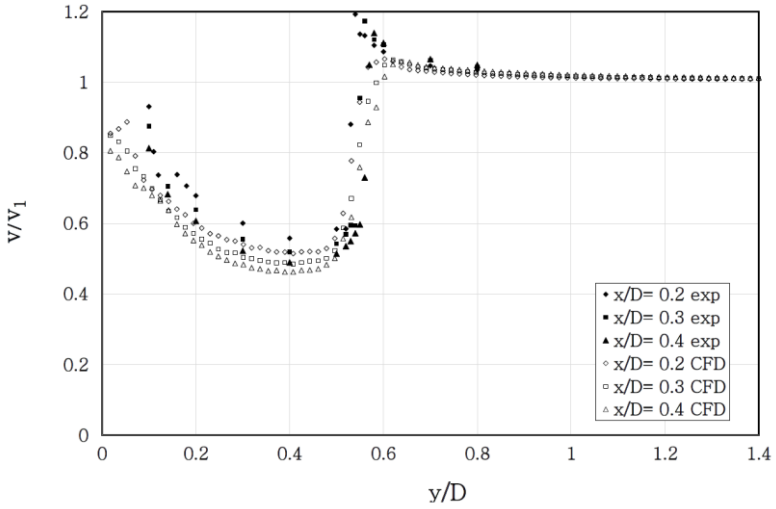

Figure 6: Axial velocity in wake of HAWT in distance of 0.2 to 0.4 diameters

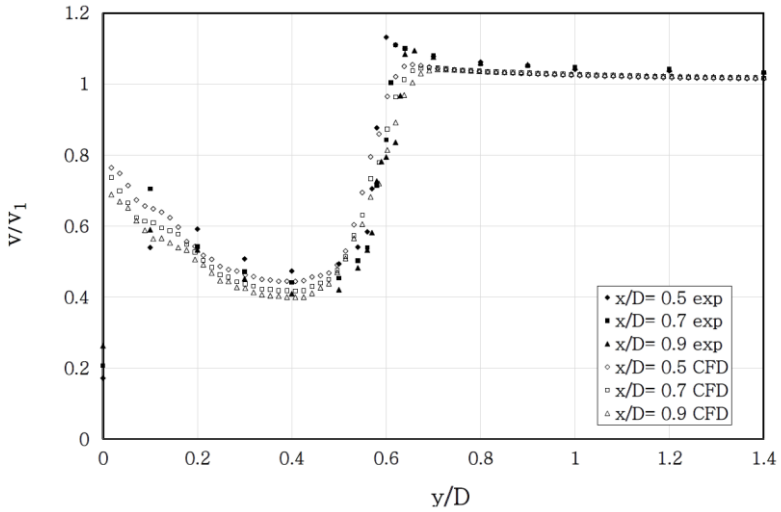

Figure 7: Axial velocity in wake of HAWT in distance of 0.5 to 0.9 diameters

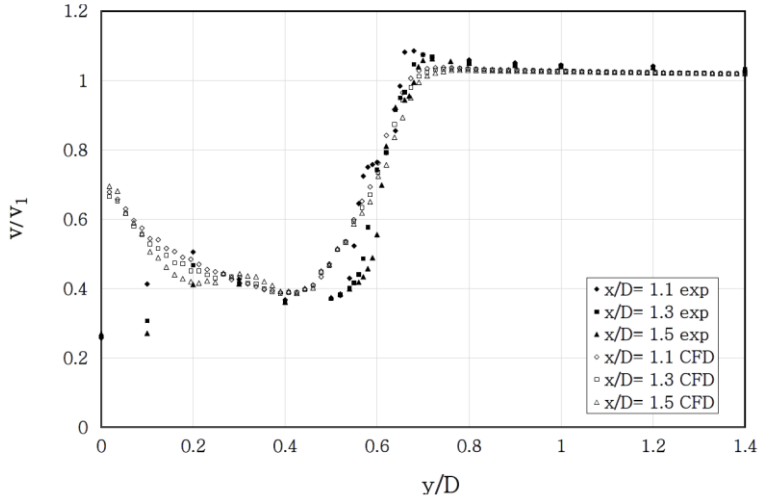

Figure 8: Axial velocity in wake of HAWT in distance of 1.1 to 1.5 diameters

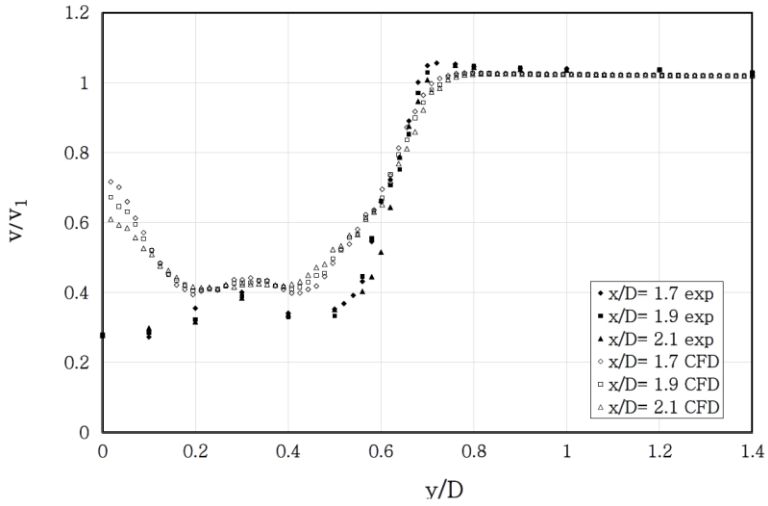

Figure 9 Axial velocity in wake of HAWT in distance of 1.7 to 2.1 diameters

Control Strategies

The turbine power at different wind velocities and control strategies are investigated. The wind velocity range is 8-16 m/s for the Fixed Speed-Fixed Pitch (FS-FP) strategy. For the Variable Speed-Fixed Pitch (VS-FP) approach the tip speed ratio is kept constant over the tested velocity range. For the Fixed Speed-Variable Pitch (VS-VP) strategy the velocity range above the design wind velocity is simulated. The same is done for the Variable Speed-Variable Pitch (VS-VP). The simulations for both of the variable pitch are performed with the variable pitch model. The rated power is set to 100W.

Figure 10 shows the power coefficient (a) and power (b) over the wind velocities for the strategies. For the VS-FP strategy the power increase with increasing of the kinetic energy in the wind.

C_P increases slightly with increasing of wind velocity, instead of staying levelled, as would be anticipated for constant tip speed ratio. A plausible explanation would be, that the increase in Reynolds number reduces separation and thus drag.
For the VP strategies the power in the high wind velocity region is levelled. Consequently the power coefficient decreases with increasing of wind velocity.

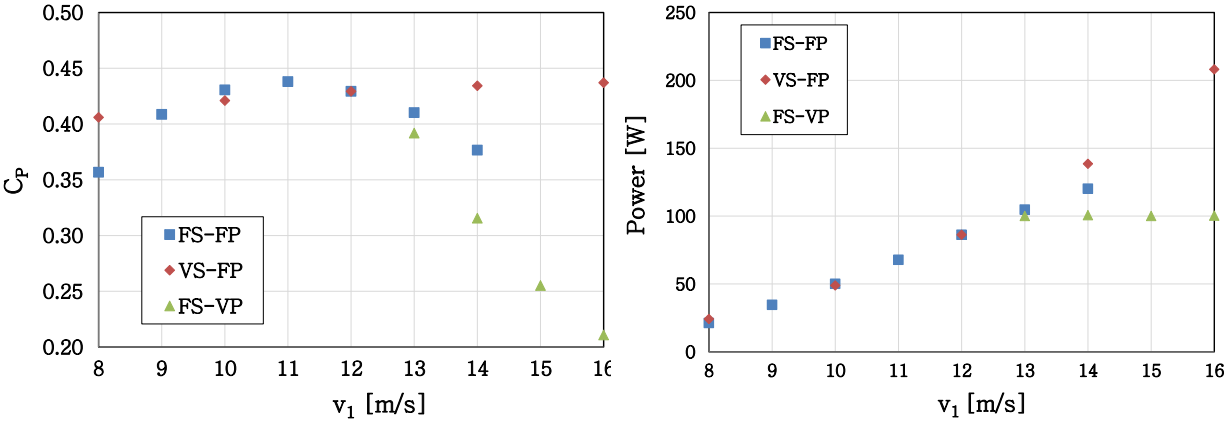

Fig. 10: Power coefficient and power over wind velocity for different control strategies

Conclusions

The aim of the present study is to perform numerical investigations for performance and wake of an optimized HAWT. The simulations are performed as steady state with the RANS k-ω SST turbulence model. The main conclusions drawn from the study are:

- The described simulation configurations can predict the performance at different operation points and clearly shows the maximum performance at the design point.
- The up-stream and down-stream axial velocities are in consistence with the experimental data.
- All control-strategies are predicted with the present CFD simulations.
- The overset technique is suitable for the variable pitch control strategy.
- Since the numerical wake analyses have been validated with the experimental data, it is possible to perform further simulations for the far-wake region which cannot be investigated experimentally.

Acknowledgment

We acknowledge the support given by the BB21 which is a collaboration project between Friedrich-Alexander University, Erlangen, Germany and Busan city, South Korea.

References

CARCANGIU, C.E.; SOERENSEN, J.N.; CAMBULI, F.; MANDAS, N.: CFD-RANS analysis of the rotational effects on the boundary layer of wind turbine blades. Journal of Physics (2007)

ANJURI, E.R.: Comparison of Experimental results with CFD for NREL Phase VI Rotor with Tip Plate. In: INTERNATIONAL JOURNAL of RENEWABLE ENERGY RESEARCH (2012)

MAHU, R.; POPESCU, F.; FRUNZULICA, F.; DUMITRACHE, Al.: 3D CFD Modeling and Simulation of NREL Phase VI ROTOR. In: Proceedings to American Institute of Physics Conference (2011)

AL-ABADI, A.; ERTUNC, O.; WEBER, H.; DELGADO, A.: A Torque Matched Aerodynamic Performance Analysis Method for the Horizontal Axis Wind Turbines. WIND ENERGY (2013)

MENTER, F.R.; KUNTZ, M.; LANGTRY, R.: Ten Years of Industrial Experience with the SST Turbulence Model. Turbulence, Heat and Mass Transfer (2003)